PREPARED FOR SUBMISSION TO JINST

Doping liquid Argon with Xenon in ProtoDUNE Single-Phase

authors

ABSTRACT: Abstract...

KEYWORDS: Only keywords from JINST's keywords list please

Contents

1 Introduction

Liquid Argon Time Projection Chambers (LArTPC) are prominent in contemporary physics for the study of neutrino oscillations and the search for rare events, including Dark Matter. This technology has been developed for more than 40 years and reached a level of sophistication that can be scaled up to multi-kilotonnes detectors. DUNE, in particular, is designing and constructing four underground modules with a fiducial mass of 10 kton each, which will be located at SURF for beam neutrino physics, atmospheric, supernove and solar neutrino detection, and for the search of proton decay. In LarTPC, the trajectories and energy deposit of charged particles is recorded by ionization losses and the correponding electron drift toward the anode. Nonetheless, Liquid Argon (LAr) is a high-performance scintillator. It emits light in the VUV region with a spectrum centered at $\lambda = 128$ nm and a yield of about 40000 photons/MeV at zero electric field and 21000 photons/MeV at the nominal electric field of DUNE: 500 V/cm. The scintillation light is produced by singlet ($\tau_s \simeq XX$) and triplet ($\tau_l \simeq XX$) de-excitations, whose ratio depends on the energy loss mechanism and can be used for particle identification by the analysis of the pulse shape.

Detecting VUV light in liquid Argon is very complex but the physics advantages are remarkable. The scintillation light localizes in time the interactions and provides the t_0 to the TPC. It then improves by one order of magnitude (1 cm $\rightarrow$ 1 mm) the location of the interaction vertex with respect to the t_0 provided by the proton kicker of the neutrino beam (LBNF for DUNE). Furthermore, light collection is the main tool to trigger events that are not produced by the beam and plays a special role in triggering and recording supernove neutrino bursts. The light is also anti-correlated with the ionization loss of the particle and can be exploited for combined charge-light calorimetry. A high light collection efficiency can outperform the TPC energy resolution, especially for low energy events.

Trapping and collection of 128 nm light is a major experimental challenge because the vast majority of materials absorbs UV light at this λ. VUV focusing is difficult and costly, and achieves limited efficiencies. In addition, the Photon Detection Efficiency (PDE) of conventional photosensors – PMTs or Silicon-Photomultipliers (SiPMs) – is extremely low even if the absorbing material is removed. In DUNE, trapping of VUV photons is achieved by a double shift complemented by a dichroic filter. The light is firstly shifted from 128 to 350 nm by a p-terphenyl (pTp) coating located on top of a dichroic filter. The filter is engineered with a 400 nm cutoff so that the shifted light crosses the filter and reaches the photon trap (ARAPUCA). A second shifter absorbs the 350 nm photons, which are isotropically reemitted at 420 mn. This can be done either through a tetraphenyl-butadiene (TPB) coating or by commercial WLS light guides. The first solution is implemented in the ARAPUCA of ProtoDUNE-SP: the demonstrator of DUNE built at CERN and operating since 2018. The second solution (X-ARAPUCA) is the most efficient one and will be implemented in the Run II of ProtoDUNE-SP and, possibly, in DUNE. In both cases, the 420 nm photons are trapped inside the photon detector because the filter is reflective above the 400 nm cutoff and reach the photosensors (cryogenic SiPMs) bouncing in the cell or, if their emission angle is smaller than the critical angle of the WLS bar, transported toward the SiPMs with practically no losses. The photosensors are located either in the bottom of the cell (ARAPUCA) or surround the border of the WLS plate.

The DUNE Photon Detection System (PDS) can be enhanced by doping LAr with Xenon at

the level of few tens of ppm. Doping became mandatory at the end of the Run I of ProtoDUNE-SP because a failure in the ricirculation system polluted the Argon with Nitrogen at the level of XX ppm. Nitrogen quenches the Ar_2^* dimers that produce the scintillation light, reducing the yield. In order to recover this loss during the run, we injected Xenon to transfer the slow component of the scintillation light (the metastable triplet state of the dimer) to the Xe before the Nitrogen quenching. Xenon light offers additional advantages, which have been investigated in literature with smaller detectors. Firstly, the Xe scintillation light is peaked at $\lambda = 178$ nm where the PDE of modern SiPMs exceed 25%. In addition, the Xe reduces the effective Rayleigh length, increasing the uniformity of light propagation without affecting the absorption length. Finally, the Xe emission is faster than the triplet emission of Ar and shorten the overall time response of the detector.

The results obtained exceeded our expectations: the yield was fully recovered with just 10 ppm of Xe without any effect on the charge collection efficiency. In addition, we benefited of ProtoDUNE-SP to perform a pilot run with Xe at different concentrations. The pilot run represents a milestone in the development of LArTPC because no large-mass detectors have ever been loaded with Xenon and the fiducial (total) LAr mass of ProtoDUNE-SP: 400 t (700 t). We then had the possibility to test the doping techniques, light yield, time stability, space uniformity and potential interference with charge collection at an unprecedented scale.

To reap this opportunity with enhanced precision, we installed an X-ARAPUCA telescope: a set of two X-ARAPUCAs located inside ProtoDUNE and triggered by plastic scintillators positioned on top of the cryostat.

This paper describes the preparation and the results of the Xe-doping run of ProtoDUNE-SP both with the the X-ARAPUCA telescope and the standard PDS. We describe these detectors in Secs. 2 and 3, respectively. The techniques to carry out a precise doping of a massive LArTPC are detailed in Sec. 4. The analysis of the data recorded by the X-ARAPUCA telescope is presented in Sec. . In this paper, we employed the entire Photon Detection System of ProtoDUNE: the ARAPUCA and the scintillation bars, both installed inside the anode planes. The results of the analysis from these detectors using an independent cosmic ray trigger are presented in Sec. 6. Finally, we used the TPC of ProtoDUNE-SP to evaluate the performance of charge collection in the presence of Xenon, as detailed in Sec. 7.

2 ProtoDUNE-SP

2.1 Detector description

2.2 Implementation of the dopant injection

Starting early 2020 , doping ProtoDUNE-SP with Xenon was performed with goals to study light yield and efficiency in the presence of Xe, long term stability and uniformity of the doped Xe inside the cryostat.

Before the doping, new photon detectors including two X-Arapucas, one fiber-pen module and an array of SIMPs were inserted into the cryostat. The mechanical assembly of these detector is shown in Figure 1. One of two X-Arapucas equipped with a quartz window which made it sensitive only to the Xe scintillation. The other X-Arapuca did not have any filter and was sensitive both to the Argon and Xenon scintillation.

A standalone DAQ system composed of an SSP and a run contral PC was also installed for data taking.

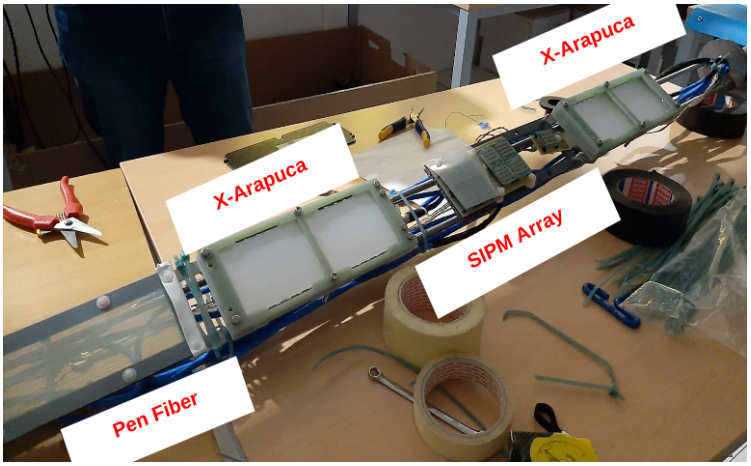

Figure 1: Additional photon detectors installed into the cryostat for Xenon studies.

Upon finalizing the preparations, xenon doping in ProtoDUNE-SP began on the 13th of February 2020 and continued over the range of five months. Xenon was injected into the warm gas circuit after the purification cartridges at a 1/1000 rate of the argon flow (which was 14 g/s at that time). The argon and xenon mixture was then condensed, passed the cold purification circuit and sent into the cryostat. The amount of doped Xe in each step and their corresponding concentrations inside the cryostat is given in Table 1.

Combining all these six Xe doping campaigns, in total 13.6 kg of Xenon was injected into the cryostat. This corresponds to 18.8 ppm of Xe concentration by mass in the 72 ton of LAr in ProtoDUNE-SP.

Extensive data taking during each injection and between the dopings was performed. The evaluation of the scintillation light and its properties inside the crystat was monitored as a function of doped Xe.

Table 1: Six Xe doping steps in ProtoDUNE-SP. The dates, doped Xe in grams and considerations in ppm by mass were given for each doping step.

Doping	**Date**	**Doped Xe[gr]**	**Doped Xe[ppm]**
1	13-14 February 2020	776	1.1
2	26-28 February 2020	2234	3.1
3	3-8 April 2020	5335	7.4
4	27-30 April 2020	3192	4.5
5	15-16 May 2020	400	0.6
6	18-20 May 2020	1584	2.2

3 The X-Arapuca telescope

The X-Arapuca (XA) telescope was inserted in the ProtoDUNE-SP TPC active volume prior the Xe doping, to measure the luminescence light yield and light pulse shape as a function of the Xe concentration, in presence/absence of the TPC electric field.

Two XA devices [1] each tuned to transmit/cut the 128 nm photons emitted by liquid Argon (LAr) luminescence, have been mounted on a ??? m long mechanical support, and inserted in the ProtoDUNE-SP detector through one of its ports, as shown in figure1, and figure 2: the telescope faces the APA-5, one of the upstream ones, at a distance of 22.7 cm (CHECK IF CORRECT).

The XA light trap is an evolution of the Arapuca design [1]; it is a reflective box equipped with an entrance window, two light downshifting stages, one dichroic filter and one lightguide coupled to SiPMs. The entrance window, coated with para-terphenyl (pTP), efficiently (>95%) downshifts photons from 128 nm to 350 nm. About 50% of the latters are isotropically re-emitted in the inner half-plane hence enter the trap that is flooded by LAr: those entering the polivinyltoluene wavelength shifting (WLS) guide (EJ286® by Eljin Co.) are isotropically re-emitted at 440 nm and, if above the critical angle, are driven to the SiPMs, located at WLS tile edges, else they leave the WLS bar. The dichroic fiter (cutoff at 400 nm) deposited on the inner side of the entrance window and the Viquiti® reflector lining the bottom and the sides of the light trap, bounce them back and forth untill they are finally either detected by SiPMs or absorbed by materials i.e. lost. The XA light collection efficiency has been independently measured at UniCamp and at INFN MiB on both a one and a two entrance window units respectively: the two measurements report an efficiency of xx ± xx % and xx ± xx % respectively.

The deployed XA devices have a frame of FR4 material, and a twofold entrance windows produced by OPTO-Electronics Co. (Brazil)[2] (95 x 75 mm^2) each, while the pTP coating is applied at UniCamp by vacuum evaporation, with a nominal thickness of ???? $\mu g/cm^2$. The WLS is a single tile of (204 x 75 x 4) mm^3, with high absorption at 350 nm and >98% emission at 440 nm [3]. The Viquiti® film guarantees high reflectivity (> 98%) at 440 nm. To cut the VUV 128 nm photons from LAr luminescence while transmitting most (85%) of the 178 nm LXe light, one of the two XAs is is equipped with an additional Suprasil® (CHECK IF CORRECT) ???? mm thick quartz window located just above the device entrance window: in the following it is referred to as Quartz-XA or Q-XA, while the other, with the exposed pTP layer is fully sensitive to 128 nm photons, is named NoQuartz X-Arapuca (NQ-XA).

The SiPMs are Hamamatsu S13360-6050VE [4] have 6×6 mm^2 active area, terminal capacitance of 1.3 nF, photon detection efficiency of 35-40% at 430 nm and are operated at 47 V bias.

In each module, 2 arrays of 4 SiPMs are positioned along each of the WLS light guide long sides (Fig.4): in each array the SiPMs are readout in parallel, resulting in a total of 4 readout channels per X-Arapuca module.

The unamplified signal of each SiPM array is delivered to the feedthrough with cat6 cables terminated with bayonet connectors. From the flange, the same cat6 cables deliver the signal to a custom "standalone" SiPM Signal Processor (SSP) module.

The SSP [5], designed by Argonne National Laboratory, consists of 12 readout channels packaged in a single module; each channel contains a fully-differential voltage amplifier and a 14-bit, 150 MSPS analog-to-digital converter (ADC) that digitizes the SiPMs waveforms. The SSP incorporate

a separate power supply for each channel, providing each SiPM board with a controllable bias, up to 60 V.
An external trigger on cosmic rays is provided by a standard triple coincidence of 15.5×44 cm plastic scintillators, located on top of the cryostat 1.15 m from the active volume, as shown in figure 3. The three paddles identify a solid angle of ????, resulting in an average trigger rate of approximately 3 Hz (*to be verified*).
For each trigger, the DAQ produces a digitized waveform for each of the 4 channels. The recorded waveform are 2000 samples or 13200 ns long, are written in an ASCII file and saved on the acquisition PC.

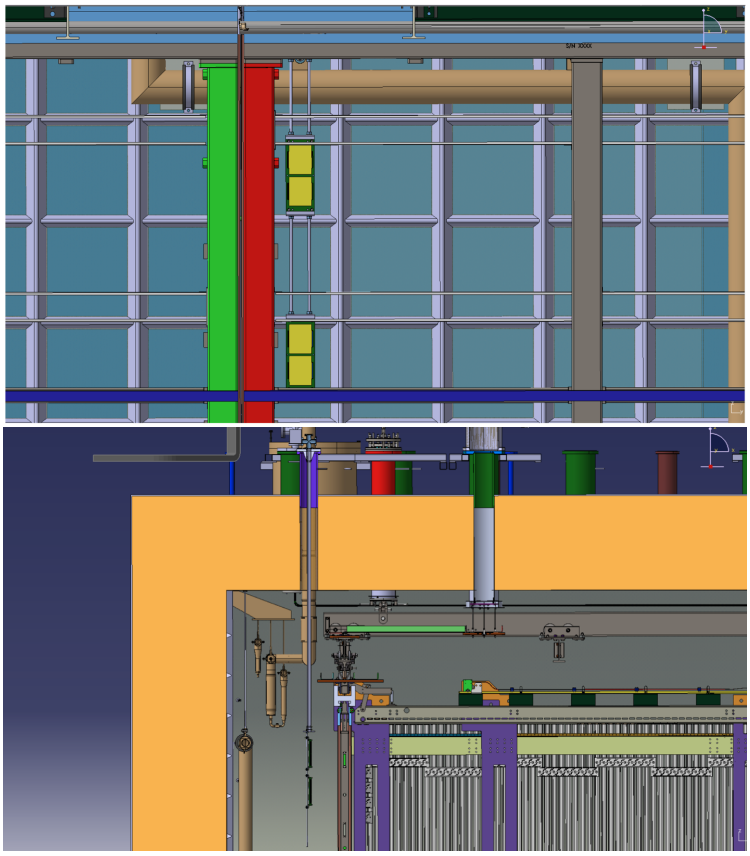

Figure 2: Top: front view of the X-Arapuca telescope inside the ProtoDUNE-SP cryostat. In green, the frame of APA-???, in red that of APA-5. Bottom: side view, showing the position of the PDS (green and light blue bars on the APA frame) with respect to the X-Arapuca.

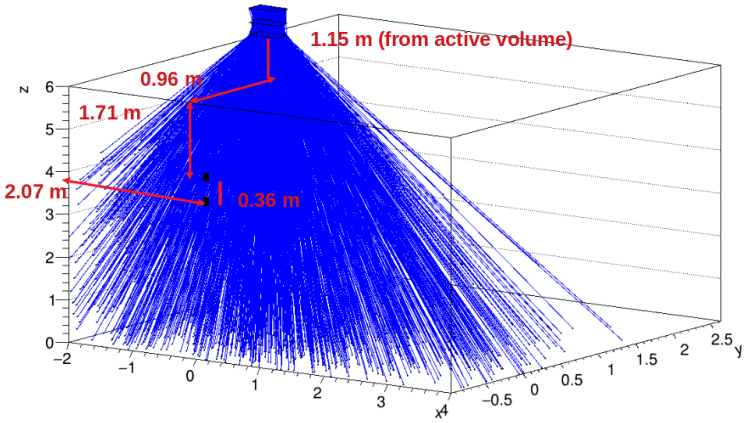

Figure 3: Position of the X-Arapuca telescope with respect to the trigger paddles.

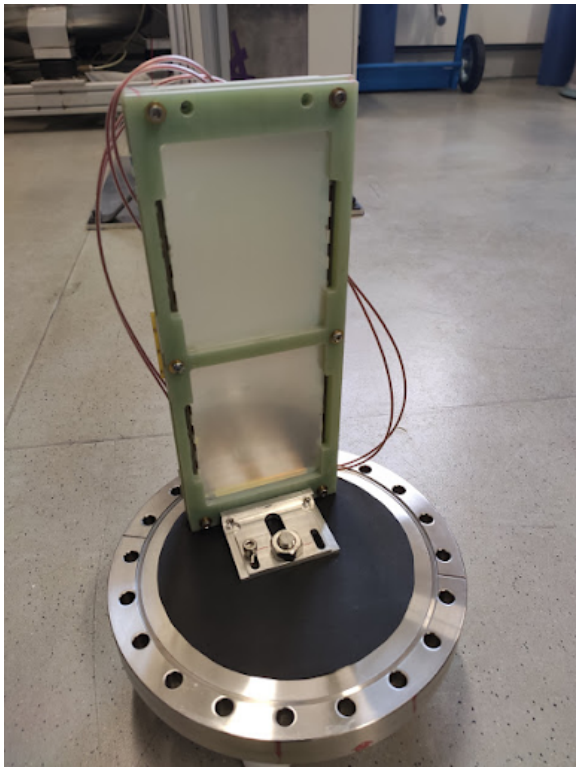

Figure 4: A closeup of one of the No Quartz X-Arapuca module.

4 The Xe-doping runs in 2020

5 Analysis of the X-Arapuca data

ProtoDUNE-SP[5, 6] is the single-phase DUNE (Deep Underground Neutrino Experiment[7]) Far Detector prototype constructed at the CERN Neutrino Platform. In January 2020, a stand-alone X-Arapuca detector was installed in the SP cryostat system. X-Arapuca[1] is the light detection system of the DUNE single phase far detector. It is composed of silicon photo-sensors (SiPMs), a reflective surface, and a cavity between SiPM and reflective surface. 127 nm photons arrive the X-Arapuca,they are converted and then reflected in the internal surface back and forth until they reach the SiPM array. X-Arapuca data acquisition was operated between February and July(during the world pandemics COVID 19) The purpose of the operation was validate the performance of the X-Arapuca detector, the performance of the liquid argon time projection chamber (TPC) and the light detection system as a function of xenon injection. Over 300 runs have been taken during the operation at different conditions, i.e. different drift field values and Xe concentrations. There were five different Xe injection eras represented by different amounts of Xe concentration in units of ppm (parts per million): 1.10 ppm, 4.20ppm, 11.60 ppm,16.00 ppm and 18.80 ppm. Two kinds of X-Arapuca were used in data taking:No window (readout channels Ch1, Ch2, and Ch3),which were sensitive to the 127 nm scintillation wavelength of liquid argon;and quartz window (readout channels Ch4, Ch5, and Ch7), which were filtering the UV light on the top of the wavelength shifter. Such a configuration can be regarded as vital in order to understand the effects of Xe concentration.

The first challenge in the analysis was the mitigation of noise. Many events were inspected individually and the source of the noise was identified to be related to the trigger electronics.In order to mitigate the noise, triggered events with no measurable signal were identified and the recorded signals were averaged. The fraction of these empty events was approximately % 7. Figure 5 hows the implementation of the noise reduction algorithm.

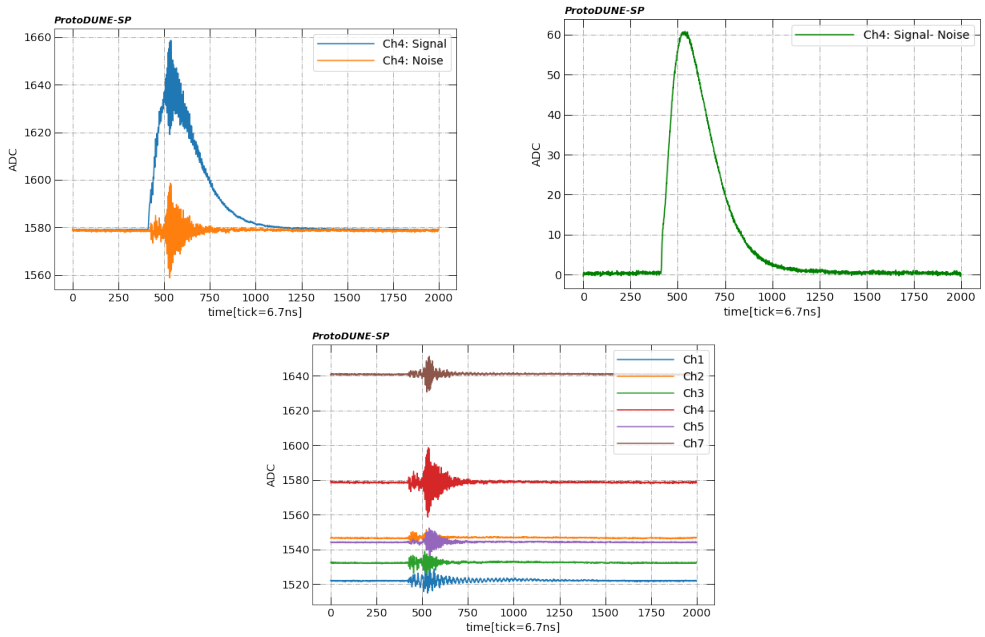

Figure 5: Top two plots implementation of the denoising

5.1 Single photo-electron calibration

The single photo-electron (SPE) was searched for in the tail of each signal, far from the trigger region for each channel, between 1100-2000 time ticks. Collected SPE charge probabilities are fitted a double Gaussian as pedestal peak and first SPE peak. The averaged SPE waveform is extracted by selecting the pulses with charge within one sigma of the mean SPE charge. This waveform serves as the impulse response for the deconvolution of the actual multi-photon pulses. Due to the shape of the SiPM signal, the timing information is washed out by the convolution of overlapping SPE waveform. Therefore, a reliable deconvolution algorithm is necessary to extract the timing information.

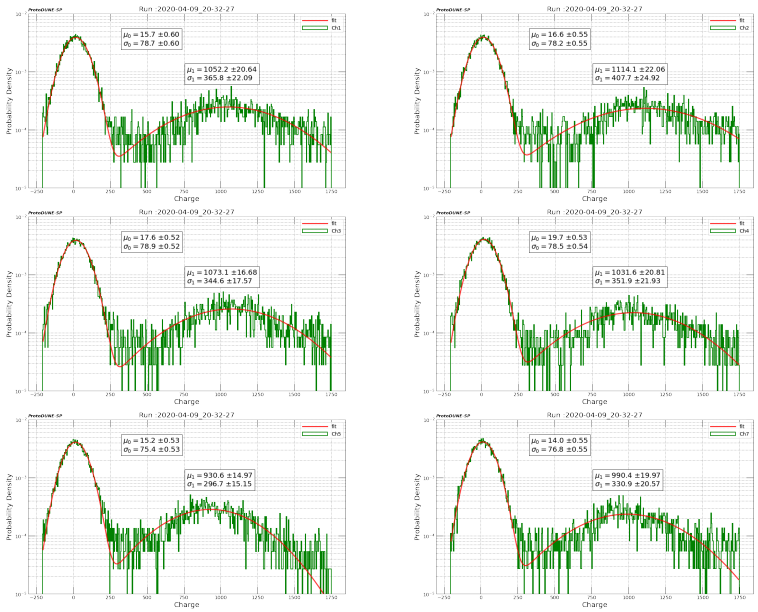

Figure 6: Charge versus probability density for each channel

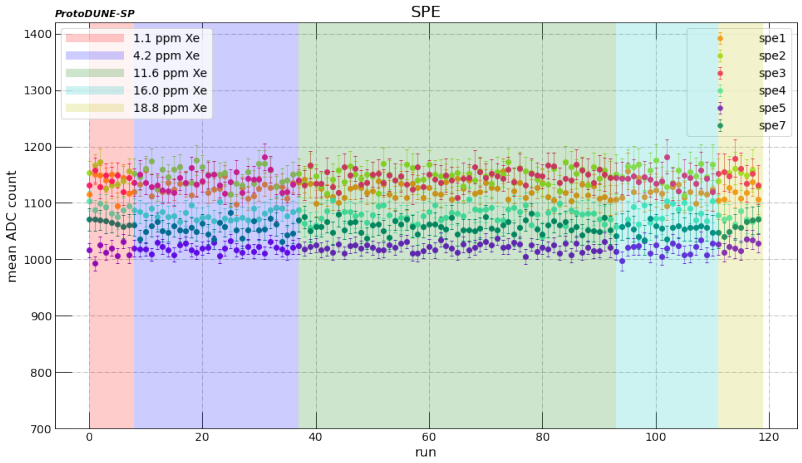

Figure 7: SPE stability

5.2 Model

First excited Ar_2^* dimer formation decay by scintillation at 128 nm, quenching through N_2, shifting to $ArXe^*$. Later $ArXe^*$ dimer formation decay by scintillation at 150 nm and shifting to Xe_2^* dimer and quenching through N_2. Finally Xe_2^* dimer disappears thought scintillation at 175 nm. Such scintillation mechanism formation can be listed in three reactions as follows;

$$Ar_2^* + Xe \rightarrow ArXe^* + Ar \tag{5.1}$$
$$ArXe^* + Xe \rightarrow Xe_2^* + Ar \tag{5.2}$$
$$Xe_2^* \rightarrow Xe + Xe + \gamma \tag{5.3}$$

$$\frac{d(Ar_2^*)}{dt} = -\frac{Ar_2^*}{\tau_{128}} - \frac{Ar_2^*}{\tau_{N2}} - \frac{Ar_2^*}{\tau_{AX}} \tag{5.4}$$
$$= -\frac{Ar_2^*}{\tau_{TA}} \tag{5.5}$$
$$\frac{1}{\tau_{TA}} = \frac{1}{\tau_{128}} + \frac{1}{\tau_{N2}} + \frac{1}{\tau_{AX}} \tag{5.6}$$

$$\frac{d(ArXe^*)}{dt} = +\frac{Ar_2^*}{\tau_{AX}} - \frac{ArXe^*}{\tau_{150}} - \frac{ArXe^*}{\tau_{N2}} - \frac{ArXe^*}{\tau_{TX}} \tag{5.7}$$
$$= +\frac{Ar_2^*}{\tau_{AX}} - \frac{ArXe^*}{\tau_{TX}} \tag{5.8}$$
$$\frac{1}{\tau_{TX}} = \frac{1}{\tau_{150}} + \frac{1}{\tau_{N2}} + \frac{1}{\tau_{XX}} \tag{5.9}$$

$$\frac{d(Xe_2^*)}{dt} = +\frac{Ar_2^*}{\tau_{XX}} - \frac{Xe_2^*}{\tau_{175}} \tag{5.10}$$

Here τ_{N2} represents the quenching due to the presence of a fixed amount of N_2 in the NP04 detector. For now, it is also assumed that the quenching effects on Ar_2^* and $ArXe^*$ have an approximately similar time constant. These equations can be solved.

$$\frac{d(Ar_2^*)}{dt}(scint@128nm) = K\frac{\tau_{TA}}{\tau_{128}}\frac{e^{-t/\tau_{TA}}}{\tau_{TA}} \tag{5.11}$$
$$\frac{d(ArXe^*)}{dt}(scint@150nm) = K\frac{\tau_{TA}}{\tau_{150}}\frac{\tau_{TX}}{\tau_{AX}}\frac{(e^{-t/\tau_{TA}} - e^{-t/\tau_{TX}})}{(\tau_{TA} - \tau_{TX})} \tag{5.12}$$
$$\frac{d(Xe_2^*)}{dt}(scint@175nm) = K\frac{\tau_{TA}}{\tau_{XX}}\frac{\tau_{TX}}{\tau_{AX}}\frac{(e^{-t/\tau_{TA}} - e^{-t/\tau_{TX}})}{(\tau_{TA} - \tau_{TX})} \tag{5.13}$$

Non Quartz window would be sensitive to sum of all three spectrum 128 nm, 150 nm and, 175 nm.

$$\frac{dXN}{dt} = K\left[\frac{1}{\tau_{128}}\frac{e^{-t/\tau_{TA}}}{\tau_{TA}} + \left(\frac{\tau_{XX} + \tau_{150}}{\tau_{XX}\tau_{150}}\right)\left(\frac{\tau_{TA}\tau_{150}}{\tau_{AX}}\right)\frac{(e^{-t/\tau_{TA}} - e^{-t/\tau_{TX}})}{(\tau_{TA} - \tau_{TX})}\right] \tag{5.14}$$

On the other hand Quartz window would be only sensitive to 175nm

$$\frac{dXQ}{dt} = K\frac{1}{\tau_{XX}}\left(\frac{\tau_{TA}\tau_{150}}{\tau_{AX}}\right)\frac{(e^{-t/\tau_{TA}} - e^{-t/\tau_{TX}})}{(\tau_{TA} - \tau_{TX})} \tag{5.15}$$

Argon and Xenon scintillation mean-life has contributed to the slow component, so double exponential decay function would be fit both X-Arapuca window. Although known argon scintillation fast component, it is observed that quartz window has a fast feature. So in total, both X-Arapuca windows represent the three exponential decay function. Figure [8] indicate three exponential decay fit results for five different Xe concentration on non-quartz and quartz window.

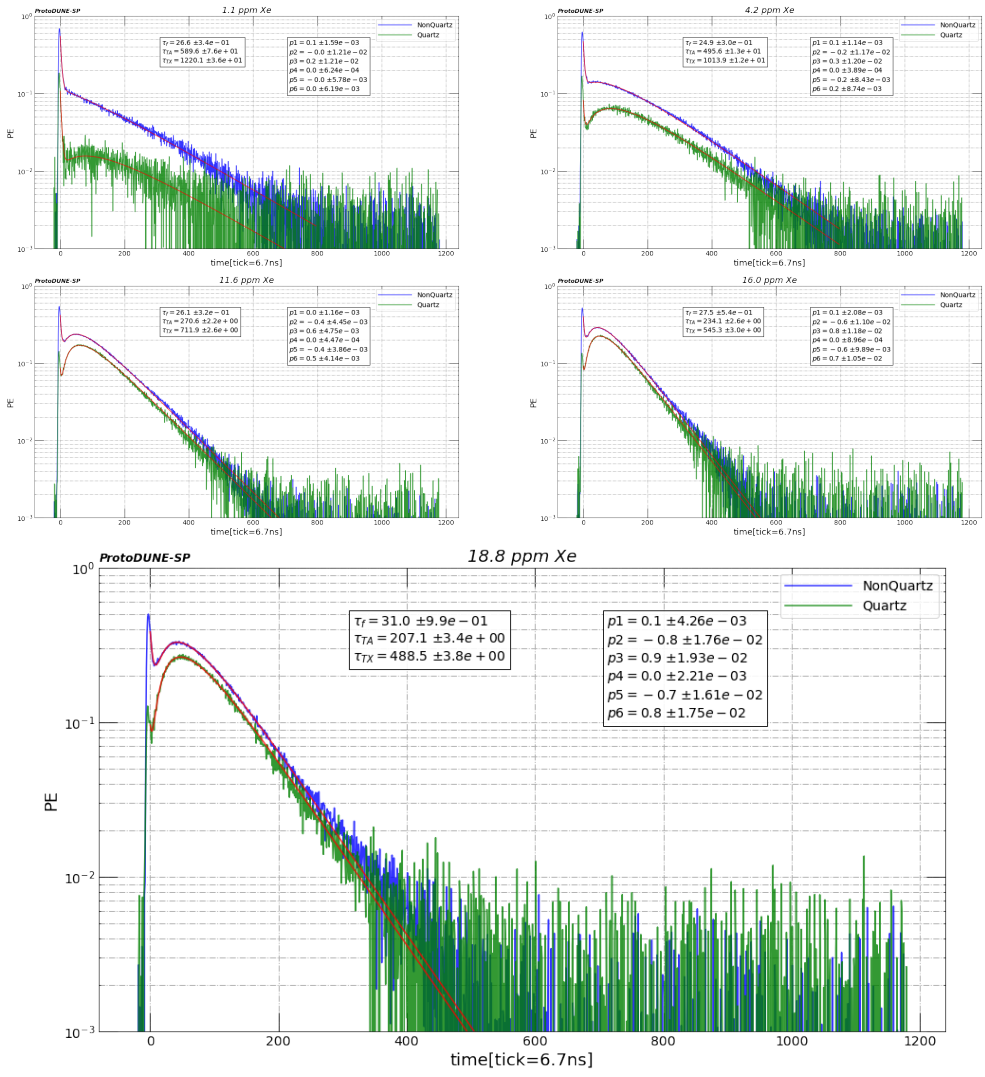

Figure 8: The simultaneous fit of the quartz window and no window average signals for five Xe injection

Ratio of XQ/XN (give ref to above aquation) would be inter calibration

$$\frac{XQ}{XN} = \frac{\tau_{150}}{\tau_{XX} + \tau_{150}} \tag{5.16}$$

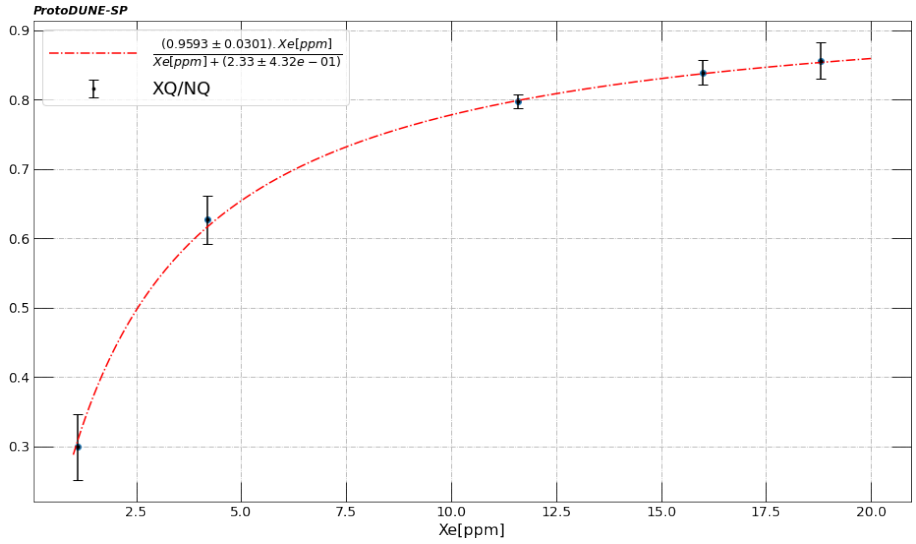

Figure 9: inter calibration between Quartz and non-Quartz window

From the simultaneous fit $1/\tau_{TA}$ and $1/\tau_{TX}$ can be plotted as a function of Xe concentrations Figure 10 and would be linear fit. Equations (5.6 ,5.9) $1/\tau_{128}$, $1/\tau_{150}$, and $1/\tau_{N2}$ does not change with Xe concentration so it will be represented with intercept of the fit.

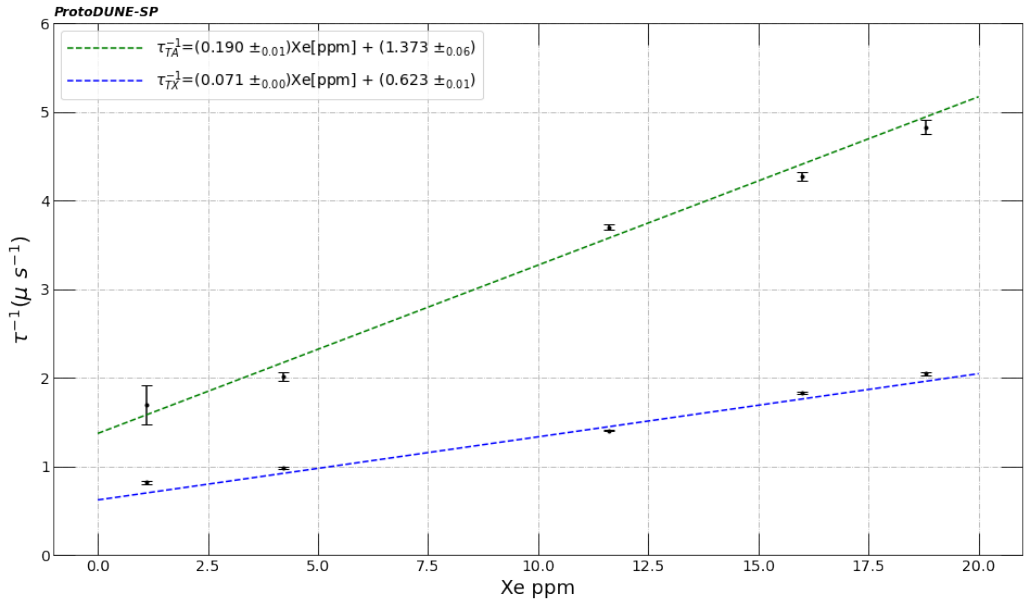

Figure 10: Ar and Xe scintillation time constant

On the other hand $1/\tau_{AX}$ and $1/\tau_{XX}$ would be depend on Xe concentration represented with slope of the linear fit.

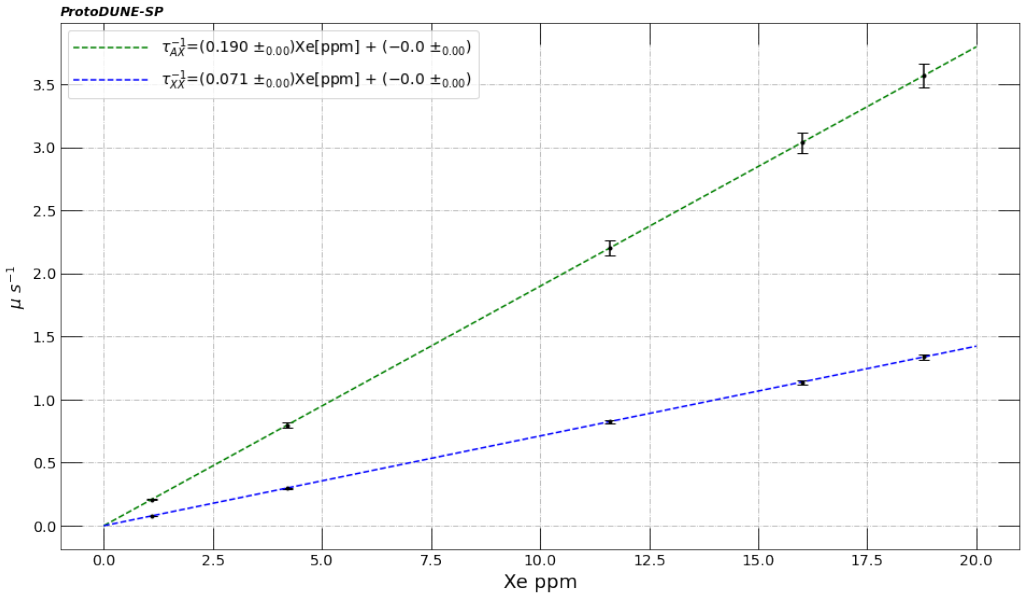

Figure 11: AX and XX scintillation time constant

Table 2: fit results.

Xe[ppm]	τ_{fast}[ns]	τ_{TA}[ns]	τ_{TX}[ns]	τ_{AX}[us]	τ_{XX}[us]
1.1	26.64 $\pm_{0.34}$	589.60 $\pm_{76.33}$	1220.08 $\pm_{35.89}$	4.79 $\pm_{0.13}$	12.77 $\pm_{0.18}$
4.2	24.91 $\pm_{0.30}$	495.57 $\pm_{12.77}$	1013.93 $\pm_{12.17}$	1.25 $\pm_{0.03}$	3.34 $\pm_{0.05}$
11.6	26.09 $\pm_{0.32}$	270.59 $\pm_{2.21}$	711.85 $\pm_{2.58}$	0.45 $\pm_{0.01}$	1.21 $\pm_{0.02}$
16.0	27.52 $\pm_{0.54}$	234.10 $\pm_{2.64}$	545.28 $\pm_{3.00}$	0.33 $\pm_{0.01}$	0.88 $\pm_{0.01}$
18.8	30.99 $\pm_{0.99}$	207.13 $\pm_{3.43}$	488.53 $\pm_{3.80}$	0.28 $\pm_{0.01}$	0.75 $\pm_{0.01}$

5.3 Data selection and deconvolution

Orci varius natoque penatibus et magnis dis parturient montes, nascetur ridiculus mus. Nam id lacus sed eros rutrum fermentum vel ut eros. Etiam ante quam, euismod fringilla sollicitudin nec, pretium sed risus. Nullam volutpat mi dolor, a pharetra odio blandit eleifend. Curabitur ut nunc odio. Proin dignissim nibh a tellus gravida fermentum. Mauris mattis bibendum lacus in mollis. In quis tellus libero. Pellentesque ullamcorper mattis metus a vulputate. Duis et orci eu lorem tempor bibendum. Suspendisse ac convallis erat. Pellentesque pretium sapien et nunc elementum mattis. Praesent sit amet orci vel ipsum gravida pharetra.

5.4 Results

Orci varius natoque penatibus et magnis dis parturient montes, nascetur ridiculus mus. Nam id lacus sed eros rutrum fermentum vel ut eros. Etiam ante quam, euismod fringilla sollicitudin nec, pretium sed risus. Nullam volutpat mi dolor, a pharetra odio blandit eleifend. Curabitur ut nunc odio. Proin dignissim nibh a tellus gravida fermentum. Mauris mattis bibendum lacus in mollis. In quis tellus libero. Pellentesque ullamcorper mattis metus a vulputate. Duis et orci eu lorem tempor

bibendum. Suspendisse ac convallis erat. Pellentesque pretium sapien et nunc elementum mattis. Praesent sit amet orci vel ipsum gravida pharetra.

6 Analysis of the ProtoDUNE-SP PDS

6.1 Trigger and data selection

6.2 N2 contamination

6.2.1 Collected light shape

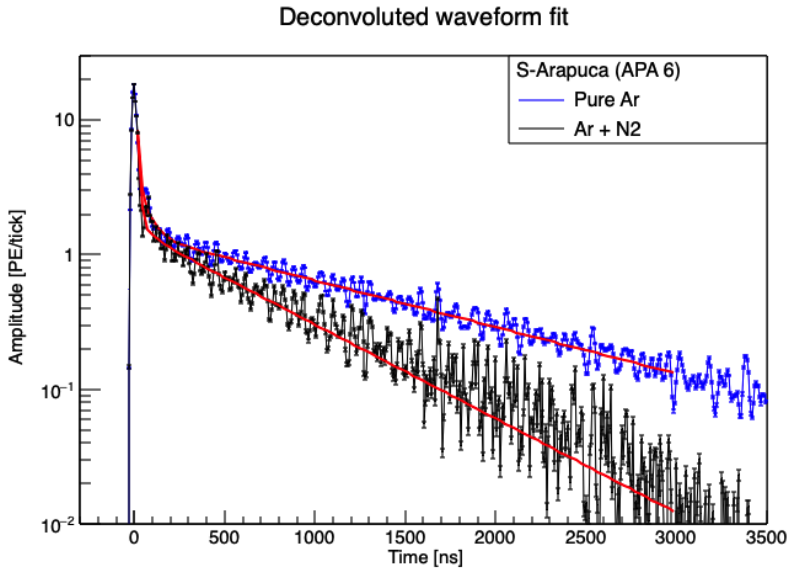

Figure 12: S-Arapuca (APA 6) deconvoluted waveforms. Blue: pure Argon (Before the Air contamination), Black: after Air contamination and oxygen purification (only N2 shoud be present).

The average waveform from each of the 12 S-Arapuca channels are deconvoluted and then summed. Figure 12 shows the Liquid Argon scintillation light shape for pure Argon and Argon plus Nitrogen contamination, both with Electric field off. The three component fit function (6.1):

$$f(t) = \frac{C_S}{\tau_S} \exp\left(-t/\tau_S\right) + \frac{C_I}{\tau_I} \exp\left(-t/\tau_I\right) + \frac{C_T}{\tau_T} \exp\left(-t/\tau_T\right) \tag{6.1}$$

shows similar results for the Singlet (τ_S) and Intermediate (τ_I) time constant, and an evident reduction for the Triplet time constant (τ_T), as expected in the energy transfer process from exited Argon to Nitrogen rate. Fit result are reported in Table 3. The pure Argon waveform is scaled to have the same maximum amplitude (Singlet amplitude) of Argon plus Nitrogen waveform.

6.2.2 Nitrogen energy transfer rate constant

6.2.3 Collected light nitrogen quenching

The main Nitrogen effect is to reduce the collected light.

6.3 Results

Fit result					
Time Constant	Pure Ar	Ar + N2	Coefficient	Pure Ar	Ar + N2
τ_S [ns]	12.72 ± 0.004	13.24 ± 0.05	C_S	209 ± 1	244 ± 1
τ_I [ns]	62.0 ± 0.5	77 ± 2	C_I	154 ± 1	299 ± 1
τ_T [ns]	1257 ± 1	621 ± 1	C_T	1790 ± 1	941 ± 1

Table 3: Parameters result from the two fits show in Figure 12. The coefficients units (not reported) are [PE] [ns/tick], where [ns/tick]=0.15.

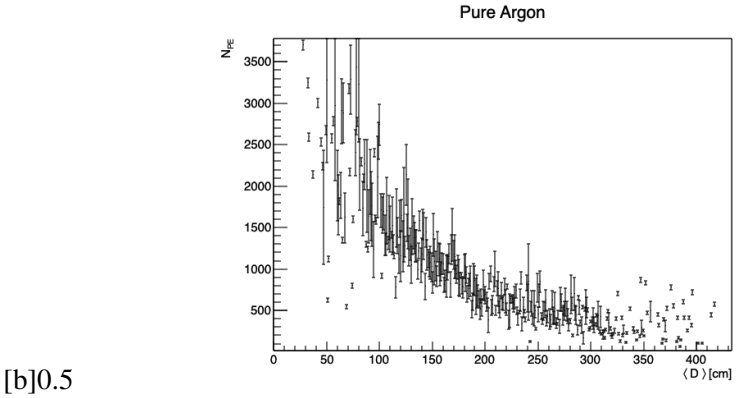

[b]0.5

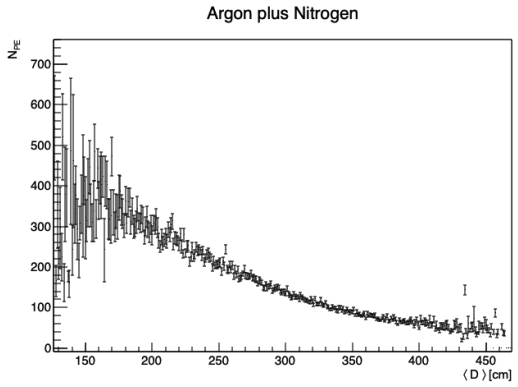

[b]0.5

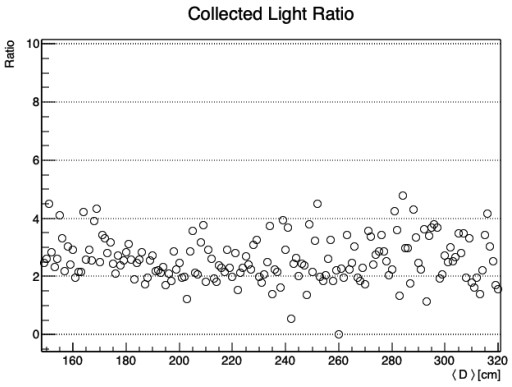

[b]0.5

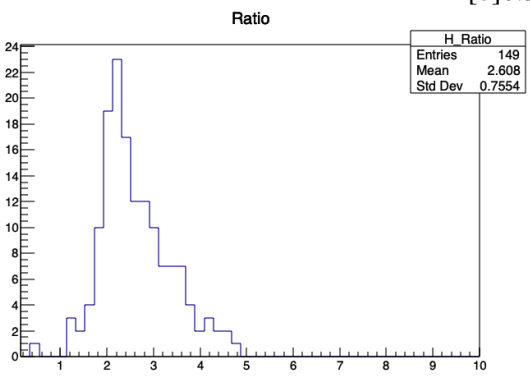

[b]0.5

Figure 13: Caption

7 Charge reconstruction in liquid Argon doped with Xe

8 Conclusions

Nulla facilisi. Duis et massa ornare, porta turpis vitae, venenatis sem. Phasellus risus ante, volutpat sed congue at, rutrum vitae arcu. Praesent efficitur tellus in risus mattis, eget fermentum nibh imperdiet. Suspendisse tempor, dui sit amet sodales tincidunt, ex diam ornare quam, quis dignissim arcu enim vel orci. Morbi a justo tempor, finibus tortor non, bibendum est. Donec ac lectus in ante tempus consectetur. Ut at sem sapien. Integer sed ex et lorem interdum laoreet. Vestibulum ut leo in diam venenatis faucibus aliquam quis massa.

References

[1] A. Machado et al., "The x-ARAPUCA: an improvement of the ARAPUCA device", *Journal of Instrumentation* **13** (apr, 2018) C04026–C04026, doi:10.1088/1748-0221/13/04/c04026.

[2] "OPTO webpage". http://opto.com.br/.

[3] Eljen Technology, "Wavelength Sifting Plastics EJ-280, EJ-282, EJ-284, EJ-286", https://eljentechnology.com/products/wavelength-shifting-plastics/ej-280-ej-282-ej-284-ej-286.

[4] Hamamatsu, "MPCC S13360-2050VE/3050VE/6050VE", https://www.hamamatsu.com/eu/en/product/type/S13360-6050VE/index.html.

[5] DUNE Collaboration Collaboration, "The Single-Phase ProtoDUNE Technical Design Report. The Single-Phase ProtoDUNE Technical Design Report", Technical Report FERMILAB-DESIGN-2017-02, Jun, 2017. 165 pages, fix references, author list and minor numbers.

[6] B. Abi et al., "Volume i. introduction to DUNE", *Journal of Instrumentation* **15** (aug, 2020) T08008–T08008, doi:10.1088/1748-0221/15/08/t08008.

[7] DUNE LBNF. https://lbnf-dune.fnal.gov/.